Multifunctional carbon black engineered cementitious composites for the protection of critical infrastructure

M. Li, V. Lin, J. Lynch and V.C. Li

Department of Civil and Environmental Engineering, University of Michigan, USA

Abstract. A new generation of self-sensing structural materials that can provide spatially distributed sensing of material damage is being developed in the context of structural health monitoring and protection of deteriorating concrete infrastructure. Engineered Cementitious Composites (ECC) doped with carbon black (CB) nano-particles are proposed as highly damage-tolerant materials whose electrical properties can be correlated to strain and cracking. Specifically, this study investigated the effect of CB dosage on the CB-ECC rheological, mechanical and electrical properties. The results show the promise of CB-ECC as a new multifunctional material that combines damage tolerance with damage self-sensing capabilities; both contribute to infrastructure safety and serviceability.

1. Introduction

The deterioration of large-scale infrastructure is a critical national problem that, left unchecked, will continue to lead to catastrophes like the I-35W Bridge collapse under service loads [1]. Deterioration will also increase structural vulnerability to man-made and natural hazards, if not detected and repaired in a timely fashion. This problem is further compounded by the shrinking of economic and natural resources needed to maintain civil infrastructure at an alarming rate [2].

Two major contributors to this compelling problem are inadequate material performance and the limitations of current structural health monitoring (SHM) approaches. Concrete materials are susceptible to cracking and fracture failure due to their inherent brittleness, which also lead to other common deterioration mechanisms such as embedded steel corrosion. Transverse cracking in bridge decks is one of the dominant deterioration problems in many States in the U.S. [3], Freeze-thaw cycles of water in cracks and leakage of water to supporting structures can reduce the bridge service life. Cracks also accelerate chloride penetration into the concrete and initiate corrosion of reinforcements, especially in marine environments or regions where deicing salts are applied in winter. The U.S. spends about $8.3 billion annually to directly address corrosion in highway bridges [4]. Indirect

costs related to traffic delays and productivity losses exceed 10 times the direct cost of maintenance/repair/rehabilitation.

While detecting damage or deterioration in concrete structural components is critical, current infrastructure management practices have relied on bi-annual visual inspections that can be subjective and limited to accessible locations [5]. While great technological advances have been made in recent years on many fronts in the SHM field, there still remain very few implementations of SHM systems in operational structures [6]. The key flaws include: indirect damage sensing that needs physics-based models to correlate structural response measurements to damage state; point-based sensors (e.g. strain gages, thermal couples, accelerometers) that cannot accurately identify spatially distributed damage; and tethered monitoring systems that require wires, often kilometers long, to connect sensors to a central data repository, leading to expensive installation and maintenance.

This research aims to address these limitations through the realization of multifunctional materials with intrinsic damage tolerance as well as distributed damage self-sensing capacity; both characteristics are essential for enhancing infrastructure resilience, reducing maintenance needs and life cycle impacts, and improving user experience. The beauty of this self-sensing multifunctional material is twofold. First, it serves as a major material component for structures to significantly improve resistance to deterioration and damage (*e.g.* cracking, corrosion and cover spalling), by eliminating concrete brittleness and intrinsically controlling crack width to a small scale. Second, it offers the capability of distributed and direct sensing of damage wherever the material is located, by exhibiting changes in electrical properties due to mechanical (*e.g.,* strain and multiple cracking) stimulus.

Resistivity of cementitious materials has been explored as a sensing functionality for hydration monitoring, composition assessment, and currently as an emerging method for measuring mechanical state. Cementitious materials are semiconductors with bulk resistivity $10^3 \sim 10^8$ Ω-cm. Under an applied steady electric field, the ions in pore water are mobilized to create current. Piezoresistivity is defined as strain induced resistivity change. Seminal work by Chung [7] explored multi-point probing of plain cement matrix and cement pastes with conductive fibers, and revealed that the electrical properties of cementitious materials can be accurately correlated to their mechanical behavior. Electrical Impedance Spectroscopy (EIS) characterization of fiber reinforced cementitious composites (FRC) was first reported by Peled et al. [8], and illuminated the electrical properties of composite phases (matrix versus fiber). While previous work focused on establishing the piezoresistive behavior of FRCs with conductive fibers, this study targets at simultaneously achieving strain-hardening, crack width control and enhanced piezoresistive behavior within a single material platform. The strain-hardening response corresponds to an extended damage process (inelastic stage), which provides damage tolerance while allowing detection of microcrack damage long before unstable localized fracture occurs, so that early warning is possible. This is achieved through incorporating conductive carbon black nano-particles into the Engineered Cementitious Composites (ECC) system with non-conductive polymeric fibers to tailor composite rheological, mechanical and electrical properties.

2. Materials and processing

The CB-ECC composite material design is achieved by ingredients selection, rheology control during processing, and microstructure tailoring. The mixture proportions of three CB-ECC designs are summarized in Table 1. The dry ingredients consisted of Type I Portland cement (C), fine silica sand (S) with average and maximum grain sizes of 110 μm and 200 μm, normal Class-F fly ash (FA), REC-15 poly-vinyl-alcohol (PVA) fibers, and carbon black nano-particles (CB). The PVA fiber was 12 mm long, 39 μm in diameter, and surface-coated with 1.2% by weight of a proprietary hydrophobic agent. CB with an average particle size of 30 nm and bulk resistivity of approximately 10^{-1} Ω-cm was incorporated at increasing ratios of weight to total cementitious ingredients (cement plus fly ash) of 0.25%, 0.5% and 1%.

Table 1. Mix compositions by weight ratio of cement

#	C	FA	S	CB (%)	W	SP	PVA (vol%)	Initial Resistivity (ohm-cm)	Gage Factors Elastic	Gage Factors Inelastic
CB-ECC -0.25%	1.0	1.2	0.8	0.55	0.60	0.013	2.0	-	-	-
								6.489×10^6 (1yr)	14.9 (1yr)	187.3 (1yr)
CB-ECC -0.5%	1.0	1.2	0.8	1.1	0.60	0.016	2.0	5.597×10^4 (28d)	44.4 (28d)	376.5 (28d)
								5.623×10^6 (1yr)	21.5 (1yr)	696.0 (1yr)
CB-ECC-1.0%	1.0	1.2	0.8	2.2	0.60	0.022	2.0	9.579×10^4 (28d)	23.8 (28d)	202.2 (28d)
								1.294×10^6 (1yr)	133.6 (1yr)	672.6 (1yr)

The mixtures were prepared in a Hobart mixer with dry ingredients mixed first. Water (W) and super-plasticizer (SP) were then added and mixed until homogeneous cement slurry with controlled rheology was formed. PVA fibers were then slowly added and mixed until uniform dispersion. The mixtures were cast into 152.4 mm × 76.2 mm × 12.7 mm tensile specimens, covered with plastic sheets, and demolded after 24 hours. They were first cured in plastic bags at 95 ± 5% RH, 20 ± 3°C for six additional days and then left to cure in laboratory air under at 20 ± 5% RH and 20 ± 3°C until the age of 28 day or 1 year for testing.

The sample specimens are shown in Fig. 1. Specimens with higher carbon content were darker colored. Under optical microcopy and high magnification scanning electron microscopy, the matrix phase appears homogeneously black with no CB aggolomeration found, indicating good CB dispersion (Fig. 2).

Introducing a large volume of 30 nm porous CB into the ECC system created significant processing challenges in terms of material workability and dispersion of PVA fibers. To address this, the amount of water and superplasticizer was optimized to achieve a homogenous slurry with plastic viscosity ranging from 7.67 Pa.s to 10.25 Pa.s and yield stress ranging from 5.47 Pa to 128 Pa, as measured by a rheometer, which allowed proper fiber dispersion and workability. To examine fiber dispersion, florescence microscopy was adopted to detect PVA fibers and their distribution at the specimen cross section. Through controlling plastic viscosity above the minimum requirement [9], good fiber dispersion was achieved, indicated by the fiber dispersion coefficients α that are in the range of 0.79-0.83 ($0 < \alpha \leq 1$; $\alpha = 1$stands for perfectly uniform fiber dispersion). The α was

determined based on an image analysis method applied to the flurescence image [9, 10]. However, reduction of total fiber number at the cross section was found for CB-ECCs compared with ECC with no CB, meaning that the high viscosity led to larger entrapped air pores that reduced the net cross section area.

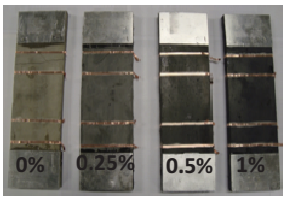

Fig. 1. CB-ECC Specimen

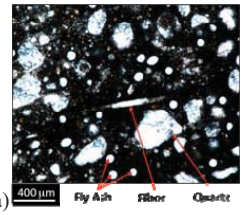

a)

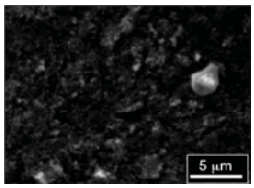

b)

Fig. 2. CB-ECC-1.0% (a) Optical Microscopy (b) Scanning Electron Microscopy

3. Mechanical and electrical properties

The composite tensile stress-strain response was tested by an Instron machine. Two LVDTs were attached to the specimen with gage length of 100 mm (Fig. 3) to measure tensile strain. The load was applied under displacement control at a rate of 0.05 mm/min during the material elastic stage and 0.5 mm/min during the inelastic stage.

The composite resistivity was measured using the four-point electronic impedance spectroscopy (EIS) method (Fig. 3). EIS is an electrical testing technique that can be used to characterize the frequency dependent electrical properties of materials and their interfaces. Four electrical contacts, i.e. copper tapes, were applied onto the surface of each specimen with highly conductive silver colloidal paste. The outer electrodes passed current into the specimen, while the inner electrodes measured the in-situ voltage within the gage length. The resistivity measurements were carried out using the Solartron 1260 impedance/gain-phase analyzer, in which the excitation voltage was set at 100 mV.

It was observed that the bulk resistivity decreased as CB content increased, which was most prominent at the lower input current frequency (Fig. 4). This identified the effectiveness of CB in increasing bulk material conductivity, and the optimal range of excitation current frequency for sensing. Consequently, the input current was fixed at 100 Hz for the composite piezoresistive response testing.

Fig. 5 shows the mechanical and piezoresistive response of CB-ECCs at 28d and 1yr ages. The tensile stress-strain curve contains three stages: (1) elastic before multiple cracking occurs, (2) strain hardening accompanied by multiple cracking process, and (3) tension softening corresponding to failure localization at one of the cracks. When the final failure occurred outside the gage length for some of the specimens, the tension softening part of the stress-strain curve exhibited a strain reduction due to the stress relaxation of the segment within gage length.

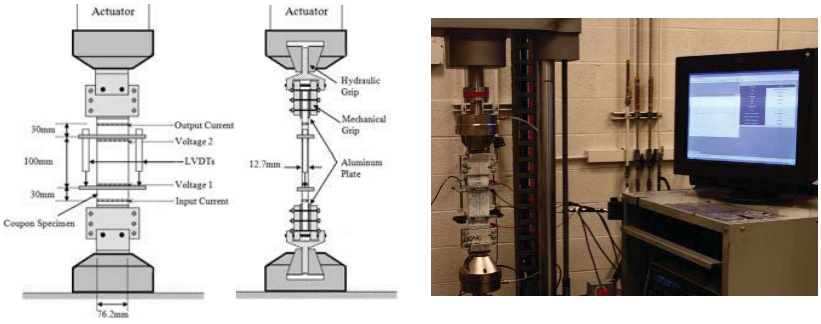

Fig. 3. 4-point EIS for piezoresistivity measurement under uniaxial tensile loading

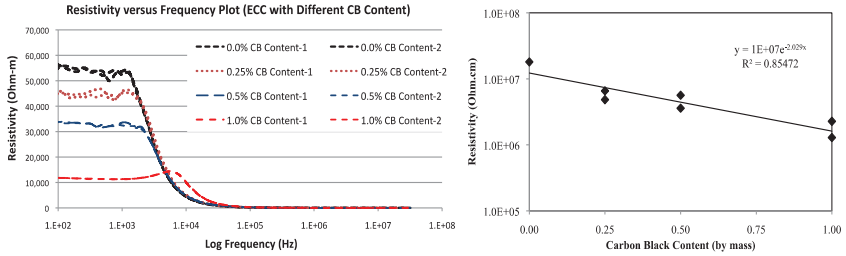

Fig. 4. 1-year-old CB-ECC Bulk Resistivity (a) vs. Frequency; (b) vs. Carbon Black Content

While all CB-ECCs showed strain hardening and multiple cracking behavior, their tensile strain capacity was in the rage of 0.8-1.8%, which were lower than typical ECCs with strain capacity of 3-5%. This reduction was due to two reasons: (1) the reduction in average crack width during multiple cracking process. It was found that the average crack width of CB-ECCs was 30-40 μm (during loading), while the average crack width of a standard ECC (ECC M45) is 60-70 μm. Single fiber pullout tests revealed enhancement of fiber/matrix interfacial bond due to the presence of CB nano-particles, leading to the reduction of average crack width. (2) The reduction of number of fibers, revealed by fluorescence microscopy at the final failure ("weakest") cross section, had led to a reduction of fiber bridging capacity. This is caused by the increase of plastic viscosity at fresh state when a large volume of porous and nano-size CB was incorporated. The detailed discussion on the experimental measurement of micro-parameters (e.g. interfacial bond), rheology and fiber dispersion, and their effects on the hardened CB-ECC composite tensile properties, will be included in a separated journal paper.

The tensile strain capacity of CB-ECCs, despite the reduction, is approximately 100 times larger than that of concrete or FRCs, and one-two order magnitude higher than shrinkage strain of cementitious materials. Shrinkage is considered to be the major cause of concrete deck cracking [3], which can be suppressed by the tensile ductility of CB-ECC [11]. Furthermore, the reduction in average crack width is favorable for resisting chloride penetration through the CB-ECC cover to reach the reinforcement and initiate corrosion [12]. It also promotes self-healing capacity [13, 14]. Through achieving tensile ductility as well as controlling crack

width to a smaller scale, the CB-ECCs possess damage tolerance for structural components to remain "healthy" under non-severe service conditions.

The bulk resistivity of CB-ECCs was two-order magnitude higher at 1 year than 28 days. This increase in resistivity with hydration process was due to the self-desiccation, and the change in concentration ions and their mobility through a tortuous path around and through the cement gel.

The CB-ECCs exhibited prominent piezo-resistive behavior, with resistivity change strongly positively correlated to strain change at both ages of 28 days and 1 year. The resistivity increase was slower during the elastic stage due to the change in the energy band gap between its valence and conductive band at low strain levels[20], and became significantly faster during the inelastic stage because the formation of microcracks separated the conductive path. Gage factors (Table 2) were used to quantify the correlation, defined as $\Delta R/R_G\varepsilon$, where ΔR is the change in resistivity caused by strain, R_G is the resistivity of unreformed gage, and ε is strain. The results confirmed that increasing CB content was effective in increasing gage factors of CB-ECC at elastic stage due to the increase in bulk material conductivity. However, the gage factor increasing trend was not clear for the inelastic stage based on the preliminary data. This suggested that multi-cracking pattern and process played a critical role on gage factors in the inelastic stage, at which the increase of CB-ECC resistivity under uniaxial tension should be due to the combined effects of matrix elastic straining, formation of new cracks, enlargement of previously-formed cracks, and crack propagation (e.g. an edge crack turns into a full crack). While the multiple cracking process depends on natural flaw distribution within the specimen, the randomness of flaws entrapped during CB-ECC processing can cause variation in the resistivity-strain curves.

To further understand the effect of cracking

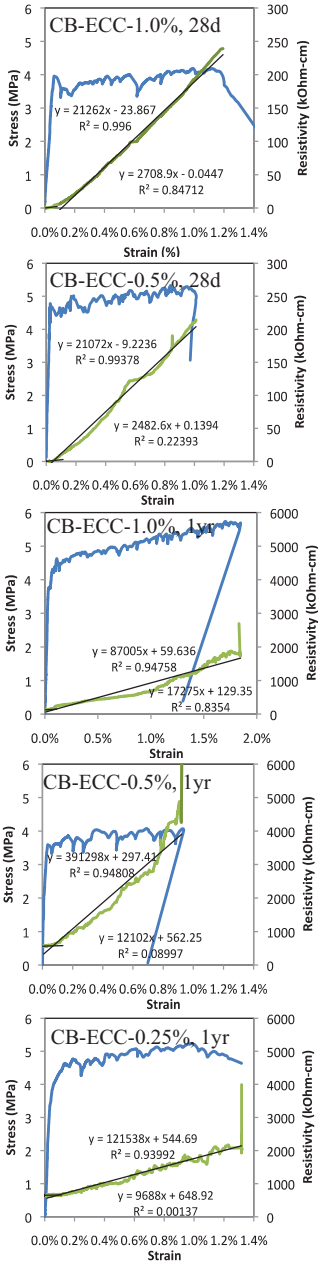

Fig. 5. Tensile stress-strain curve and resistivity-strain curve of CB-ECCs

behavior on the resistivity and strain changes, 78 images of the cracking pattern of the CB-ECC-1.0% specimen during uniaxial tensile testing was taken at fixed time intervals. Each image was analyzed to count crack number at corresponding strain level, based on the assumption that each edge crack was considered as a single crack. The relation between crack number, tensile strain and resistivity is plotted in Fig. 6. Approximately linear relation was shown between tensile strain and crack number, with a slope suggesting 39 μm average crack width during multiple-cracking process, which corresponds well with the observation using a microscope during testing. The correlation between resistivity and crack number is non-linear, indicating a non-uniform multiple cracking process, e.g. unequal width of microcracks formed at lower strain vs. higher strain levels, full crack vs. edge crack, and networking of cracks. With more tests conducted in future to establish the correlation between resistivity with cracking pattern, such correlation can be used for damage sensing.

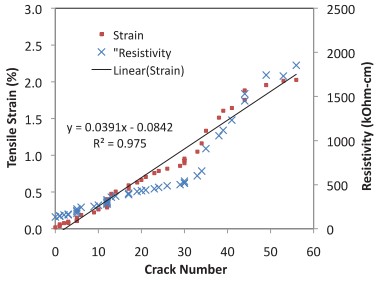

Fig. 6. Correlation between tensile strain, resistivity and crack number

4. Conclusions

This study shows the promise of CB-ECC as a multifunctional infrastructure material with damage tolerance and self-sensing capacities, both are important for the protection of critical infrastructure. By incorporating CB nano-particles into the ECC system through rheology control, the CB-ECC achieved adequate workability, close-to-uniform PVA fiber and carbon black dispersion, reduced bulk resistivity by one magnitude, strain hardening behavior with tensile strain capacity of 0.8-1.8% that is essential for resisting shrinkage cracking, and reduced crack width to 30-40 μm during loading state that provides resistance to chloride penetration. All CB-ECCs exhibited prominent piezoresistive behavior, with increasing resistivity with increasing tensile strain and cracking number, indicating the potential of CB-ECC for strain and damage sensing.

CB-ECC's lower tensile strain capacity than typical ECCs was due to the larger entrapped air pores that reduced the fiber bridging capacity at the final failure cross section, and the tighter crack width as a result of CB's effect on improving fiber/matrix interfacial bond. To reduce larger pores, the optimization of material ingredients, proportion and rheology is suggested for future studies.

While the gage factors have been determined for both the elastic and inelastic stages of CB-ECCs, more experimental studies are necessary to accurately establish the correlation between resistivity change and strain as well as cracking pattern, and to fully understand the effect of the multiple cracking process on the variation in gage factors. This includes characterizing the resistivity change under a

single crack opening scenarios with different stress-crack opening relationship, and the resistivity change under various multiple cracking processes caused by the randomness of flaw distribution. Future studies will also focus on the effect of environmental factors on gage factors, and optimizing CB-ECC composite design to achieve robust mechanical and piezoresistive behavior.

Acknowledgement

The authors would like to gratefully acknowledge the U.S. Department of Commerce, National Institute of Standards and Technology (NIST) Technology Innovation Program (TIP) for supporting this research work.

References

[1] Wardhana, K., and Hadipriono, F. C., "Analysis of recent bridge failures in the United States", Journal of Performance of Constructed Facilities, 17 (3), pp. 144-150, 2003.
[2] Anderson, J., "Cities debate privatizing public infrastructure",The New York Times, 2008.
[3] Saadeghvaziri, M. A., and Hadidi, R., "Transverse Cracking of Concrete Bridge Decks: Effects of Design Factors", ASCE Journal of Bridge Engineering, 10(5), pp.511-519, 2005.
[4] Bavarian, B., and Reiner, L., "Migrating Corrosion Inhibitors for Steel Rebar in Concrete," Materials Performance, pp. 3-5, 2003.
[5] Rolander, D. D., Phares, B. M., Graybeal, B. A., Moore, M. E., and Washer, G. A., "Highway bridge inspection: State-of-the-practice survey", Transportation Research Record, 1749 (1), pp. 73-81, 2001.
[6] Derriso, M. M., Olson, S. E., DeSimio, M. P., and Pratt, D. M., "Why are There Few Fielded SHM Systems for Aerospace Structures?" 6th International Workshop on Structural Health Monitoring, Stanford, CA, 2007
[7] Chung, D., "Piezoresistive Cement-Based Materials for Strain Sensing", Journal of Intelligent Material Systems and Structures, (13) 599, 2002.
[8] Peled, A., Torrents, J. M., Mason, T. O., Shah, S. P., and Garboczi, E. J., "Electrical Impedance Spectra to Monitor Damage during Tensile Loading of Cement Composites", ACI Materials Journal, 98(4):313-322, 2001.
[9] Li, M., Multi-Scale Design for Durable Repair of Concrete Structures, Ph.D Thesis, University of Michigan, 2009.
[10] Lee, B. Y., Kim, J. K., Kim, J. S., and Kim, Y. Y., "Quantitative Evaluation Technique of Polyvinyl Alcohol (PVA) Fiber Dispersion in Engineered Cementitious Composites", Cement and Concrete Composites, 31 (6), pp. 408-417, 2009.
[11] Li, M., and Li, V. C., "Influence of Material Ductility on the Performance of Concrete Repair", ACI Materials Journal, 106 (5), pp. 419-428, 2009.
[12] Sahmaran, M., M. Li, and V.C. Li, "Transport Properties of Engineered Cementitious Composites Under Chloride Exposure", ACI Material Journal, 104 (6), pp. 604-611, 2007.
[13] Li, M., and Li, V. C., "Cracking and Healing of Engineered Cementitious Composites under Chloride Environment", accepted, ACI Materials Journal, November 2010.
[14] Kan, Li-Li, Shi, H. S., Sakulich, A. R., and Li, V. C., "Self-Healing Characterization of Engineered Cementitious Composites", ACI Materials Journal, 107 (6), pp.617-624, 2010.